DEUTSCHES ELEKTRONEN – SYNCHROTRON DESY

DESY SR 87-01
January 1987

ADSORPTION SITES OF BROMINE ON Si(111) 1x1 AND 7x7 SURFACES

by

P. Funke

II. Inst. f. Experimentalphysik, Universität Hamburg

G. Materlik

Hamburger Synchrotronstrahlungslabor HASYLAB at DESY

ISSN 0723-7979

NOTKESTRASSE 85 · 2 HAMBURG 52

To be sure that your preprints are promptly included in the
HIGH ENERGY PHYSICS INDEX,
send them to the following address (if possible by air mail):

DESY
Bibliothek
Notkestrasse 85
2 Hamburg 52
Germany

DESY SR 87-01
January 1987

ISSN 0723-7979

ADSORPTION SITES OF BROMINE ON Si(111) 1x1 AND 7x7 SURFACES

P. Funke*
II. Institut für Experimentalphysik der Universität Hamburg,
Luruper Chaussee 149, D-2000 Hamburg 50, FRG

and

G. Materlik
Hamburger Synchrotronstrahlungslabor HASYLAB at DESY,
Notkestr. 85, D-2000 Hamburg 52, FRG

The adsorption sites of Br on well characterized ultra-high vacuum prepared Si(111) 1x1 and 7x7 surfaces were determined with in situ X-ray standing wave measurements. Only small differences were observed for low Br coverages ($\lesssim$ 1/3 ML) between the on-top adsorption taking place on the 1x1 and the 7x7 surfaces. This is in conformity with the change of the LEED pattern and indicates a local reordering of the 7x7 unit cell. At Br coverages $\gtrsim$ 1/3 ML an outward shift of the (111) Fourier component of the Br distribution function was measured. These results are compared with models of the Si(111) surface and discussed with semi-empirical formulae for the binding.

submitted to Surf. Sci.

I. Introduction

The adsorption of halogen atoms on Si(111) has been studied in many theoretical and experimental investigations in order to determine the electronic states and the geometrical arrangement of the interface atoms. Because of the expected monovalency of the halogen atoms, this system promises to be a good case to learn in which way the chemisorption of atoms on the surface depends on the reconstruction and relaxation of the substrate and on the electronic levels and the electronegativity of the adsorbed species, and in which way such substrate properties are changed by the reaction on the surface. A systematic comparison of the adsorption going through the halogen series for example, can help to separate the influence of atomic size and electronic effects for the adsorption process.

In particular, the geometrical structure of the Br/Si(111) surface has been investigated in several X-ray standing wave (XSW) studies /1-6/. Since Br forms a stable, well ordered layer even upon chemical deposition, and since such layers show a very low desorption rate, a comparison of different preparation processes as well as different environments becomes feasible by using XSW. The surface on-top site, which is expected for a monovalent bonding of the Br to the Si dangling bond was found /2-4/ for chemisorption on a mechano-chemically polished surface from an alcohol solution.

The same preparation technique used on a cleaved surface showed at low coverages the identical result with evidence of a small outward relaxation, but additionally revealed another position with increasing coverage which agreed with a threefold ionic bonding site /6/. Independently, this later position was measured in the first XSW study carried out in situ in ultra-high vacuum on a Si(111) 1x1 surface at ~ 1 ML Br coverage /5/. This result, however, can also be interpreted with a model in which Br adsorption takes place at the on-top site on a (111) surface which is inwardly relaxed by a large amount of 0.5 Å as was suggested for the clean Si(111) 7x7 surface /7/.

In our present study we have compared the Br adsorption on 1x1 and 7x7 surfaces and have measured the position as a function of Br coverage. The results identify the influence of the adsorbate on the substrate surface order and give an estimate of the interaction of the Br at larger coverages. The question of surface relaxation has been addressed as well.

II. Experimental Techniques

We have used standing X-ray wavefields to determine the adsorbate geometry as well as the coverage of adsorbed Br atoms. The simultaneous measurement of the substrate reflectivity and the inelastically scattered adsorbate fluorescence photons can be used to determine the surface atom density function relative to a known origin in the undisturbed substrate lattice. Its application for surfaces and the mathematical procedure which is used to extract the corresponding (hkl) Fourier component of the surface atom density from the measured data of the (hkl) dynamical reflection has been described in several prior publications /6,8/ and a brief review of recent applications with synchrotron radiation is given in /9/.

The experiment was carried out at the instrument ROEMO of the Hamburg Synchrotron Radiation Laboratory HASYLAB using synchrotron radiation from the storage ring DORIS. The complete set-up including the ultra-high vacuum chamber in which the sample was prepared, characterized, and measured is described in detail elsewhere /10/. A schematic drawing is repeated in Fig. 1. Our present experimental description will therefore concentrate on the sample preparation techniques used and the characterization methods to assure that XSW can be applied to the samples.

The Si(111) samples were cut from a high resistivity (> 10^3 Ω cm), p-type single crystal with a size of 10 x 5 x 5 mm^3. They were mechanically polished to optical flatness with diamond paste, etched in a solution of 95% HNO_3 + 5 % HF and finished by a chemical-mechanical Syton polish. Just before insertion into the vacuum chamber, the oxide layer was removed in a pure HF bath. Inside the UHV, the sample was carefully heated with direct current for several hours at elevated temperatures until the normal base pressure of the system was reached again.

After this treatment the surface was usually cleaned for 30 minutes with 500 eV Ar^+ ions. The damage to the crystal lattice from this treatment was annealed again by heating the sample for several minutes at high temperatures of 1200° to 1300°C. This final temperature and the cooling rate determines whether a 1x1 or 7x7 reconstructed surface is formed at room temperature. A fast cooling rate will quench the high temperature 1x1 structure /11/ while a maximum temperature above 1300°C together with a slow heating and cooling cycle (1 - 1.5 h) produces a 7x7 surface.

The slowness of all thermal treatments, avoiding extensive thermal strains, also helped to preserve the high perfection of the substrate lattice which is used as reference for the adsorbate distribution function. Two standard X-ray diffraction techniques, double crystal diffractometry and three crystal topography were used to monitor the substrate perfection. Fig. 2 shows the influence of sputtering on the reflectivity which was measured by rocking in a parallel mode the first and second crystal relative to the third crystal which is the sample. Although the fwhm of the curve is not affected strongly, its shape has changed drastically. The plateau at the top has become more rounded and the intensity in the tails increased because of defects and strains induced from sputtering.

Fig. 3 shows topographs of the full size reflected beam from the sample. During the exposure the relative angle $\Delta\vartheta$ (Fig. 2) was kept constant at about 50 % of the maximum intensity of the rocking curve. For the top row of the rocking curve one picture was taken on the right and one on the left slope of the rocking curve. The topographs show one fringe extending across the sample which images a corresponding strain variation of the lattice constant. However, sections of the homogeneous area can be chosen for an XSW measurement. Such characterization was used in each case, and a proper perfect area for the XSW measurement was selected. The bottom picture shows an almost homogeneous reflection for comparison.

A LEED system with e^- energies between 30 and 50 eV was used to characterize the surface reconstruction. By applying a 1 kHz modulated retarding voltage to the grids of this system and operating the e^- gun at about 2 keV, it was converted into an Auger-electron spectrometer. Fig. 4 (solid line) shows such Auger-electron measurement of a sample just after insertion into the UHV. The main contaminants are C, O and N. After sputtering and heating as described above, a spectrum is recorded for which the dashed line in Fig. 4 is typical. The O and N peaks have vanished but a small amount of C is still visible which may, however, partly originate from a minute contamination of the spectrometer itself.

Br was adsorbed from an electrolytic AgBr cell /12/. The doses could be controlled via the current passing through the cell since the amount of Br released at the anode is proportional to the electric current. This value is checked and calibrated by measuring the Br K fluorescence yield in units of the Si K_α yield from the substrate /13/.

III. Data Analysis

All XSW measurements which are discussed here were performed with (111) reflection planes lying parallel to the Si surface. Thus the (111) Fourier component of the Br atomic density function is determined in our measurements relative to the bulk diffraction planes. The experimental data are fitted by a least-squares fit to the formula

$$Y(\vartheta) = 1 + R(\vartheta) + 2\,(R(\vartheta))^{1/2}\, f_c \cos(v(\vartheta) - 2\pi\Phi) \qquad (1)$$

where $Y(\vartheta)$ is the fluorescence yield, normalized to its value at an off-Bragg angle ϑ, $R(\vartheta)$ and $v(\vartheta)$ are intensity and phase of the reflected beam relative to the incident beam, calculated from the dynamical theory. In order to determine the angular scale, the measured reflectivity is convoluted with the monochromator angular emittance function and fitted to $R(\vartheta)$. f_c and Φ are the amplitude and the phase, respectively, of the (hkl) Fourier component $F_H = f_{c,H} \exp(-2\pi i \Phi_H)$ of the normalized atomic density distribution of the fluorescence selected species.

Since we detected Br K_α radiation which originates from electronic orbitals extending over a narrow range close to the Br nuclei, we can use a δ-function like Br density function /8/

$$\rho(\underline{r}) = \rho_o + \sum_j \rho_j\, \delta(\underline{r} - \underline{r}_j) \qquad j = 1, 2, \ldots, n \qquad (2)$$

with $\rho_o + \sum_j \rho_j = 1$, where n gives the number of occupied sites.

The Fourier components are

$$F_H = \sum_j \rho_j \exp(2\pi i \Phi \underline{H}\cdot\underline{r}_j) = |F_H| \exp(-2\pi i \Phi_H) \qquad (3)$$

with

$$|F_H|^2 = \sum_j \rho_j^2 + 2 \sum_{\substack{j,k \\ j<k}} \rho_j \rho \cos(2\pi \underline{H}\cdot(\underline{r}_j - \underline{r}_k)) \qquad (4)$$

and

$$\tan(2\pi\Phi_H) = \sum_j \rho_j \sin(2\pi \underline{H}\cdot\underline{r}_j) / \sum_j \rho_j \cos(2\pi \underline{H}\cdot\underline{r}_j) \qquad (5)$$

Themal vibrations can be included by modifying the density function appropriately /8/. For our analysis, a density function (2) has been used with only one Br site occupied coherently relative to Si bulk diffraction planes and the rest being uniformely distributed. Thus, a coherent fraction $f_c = \Theta_c/\Theta$, where Θ is the total coverage and Θ_c the coherent coverage of Br atoms occupying sites $\Phi_H = (\Delta d/d)_H$ measured in direction of $\underline{H}$, is determined by this analysis.

IV. Results

The result of an XSW measurement can, in addition to the LEED pattern, be used to check the homogeneity of the adsorbate structure. Table 1 shows the values of f_c and Φ obtained for different surface areas of a sample. They clearly exhibit inhomogeneities resulting from this particular preparation. Such variations in f_c and Φ can point towards adsorbate inhomogeneities as well as towards bulk substrate deformations and have to be controlled carefully before the measurement to ensure a homogeneous adsorbate.

Br adsorption on Si(111) 1x1

No change of the LEED pattern was observed when Br was adsorbed on an initially Si(111) 1x1 surface. A typical result of a preparation with Θ = 0.2 ML is shown in Fig. 5. A coherent fraction $f_c = 0.96 \pm 0.07$ is reached which proves the validity of the assumed one-position model. The position $\Phi = 0.84 \pm 0.01$ is equivalent to a distance of (2.64 ± 0.03)Å to the Br atoms from the topmost bulk (111) diffraction plane. Assuming an unrelaxed, bulk like topmost Si atomic plane and Br adsorption at the one-fold covalent atop site, this result is in very good agreement with the bond length observed in $SiBr_4$ molecules (2,54 Å) /15/, with theoretical cluster calculations (2.62 Å) /16/ and with XSW measurements on chemically prepared interfaces under atmospheric conditions (2.61 Å) /4/.

To determine the influence of the Br-Br interaction the Br coverage was increased up to 1 ML. Table II gives a summary of the results from a consecutive run on the same sample spot. As can be seen, the phase value increases with coverage. Above $\Theta \approx 0.3$ ML the phase becomes 0.88 ± 0.01 while the amplitude is not affected strongly.

Fig. 6 shows the result of tempering a Br covered sample (0.5 ML) at about 300°C. The phase changes by the same amount as in the case of increasing the thickness of the Br layer. However, in the case of heating the amplitude also increases. While the total coverage decreases as expected from thermal desorption, the coherent coverage increases from 0.12 ML to 0.18 ML, which reflects the thermal annealing of the layer.

Br adsorption on Si(111) 7x7

When Br was adsorbed on a 7x7 reconstructed Si(111) surface, the LEED pattern changed markedly. Except for those seventh order LEED spots along the lines connecting the first order spots in the form of a hexagon and a six-fold "star" around each first order spot, all other fractional order spots vanished. The new pattern is similar to that observed after Cl and H adsorption on 7x7 /17,18/.

Fig. 7 (solid line) shows the result of an XSW measurement with Θ = 0.24 ML after Br deposition at room-temperature. The phase value Φ = 0.82 ± 0.01 is hardly significantly different from that of adsorption onto a 1x1 reconstructed surface. Adsorption onto 7x7 with Θ = 0.42 ML gave the identical phase value with a slightly reduced f_c = 0.76 ± 0.03. The dot-dashed line shows the results after tempering the adsorbate at 300°C. The phase Φ = 0.81 ± 0.01 is not significantly different from the results of the 7x7 surface. The coherent coverages Θ_c decreased from 0.20 ML to 0.13 ML and the LEED pattern changed fully to 1x1.

In this measurement the theoretical coherent fraction f_c^{Si} = 0.71 from the substrate Si atoms was reduced by imperfection to 0.61 ± 0.03. If this difference is applied as correction for inhomogeneities of the Br adsorbate caused from substrate imperfections, f_c values close to the theoretically maximum possible value which is the Debye-Waller factor of the Si-Br system are reached.

V. Discussion

Because of the large coherent fractions which were measured for the Br on 1x1 and 7x7 surfaces and which are close to the maximum possible value, the assumption, that Br occupies at low coverages one adsorption site has been unambiguously justified. Several measurements gave high coherent fractions

with identical positions for each kind of reconstruction and only very small differences between 1x1 and 7x7.

Table III compares the measured distance of the Br atom relative to the topmost bulk (111) diffraction plane with other relevant values. We have also included a semi-empirical estimation /19,20/ using the equation for the bondlength d_{cov} in a covalent bonding

$$d_{cov} = r_{Si} + r_{Br} - c\,|\chi_{Si} - \chi_{Br}| \qquad (6)$$

of two atoms with covalent radii r_{Si} = 1.17 Å and r_{Br} = 1.14 Å and electronegativities χ_{Si} = 1.8 and χ_{Br} = 2.8. The later difference is the measure for the shortening of the bonding arising from the different electronegativities of the partners; the constant c = 0.06 Å was taken from ref. /19/.

The agreement between the result of equ. (6), the cluster calculation, the XSW result on chemically prepared adsorbates, and the XSW UHV result on an initially 1x1 reconstructed surface is excellent.

The Φ-results on the system which was originally 7x7 reconstructed are slightly smaller. The maximum relaxation which is in agreement with the results, is the difference between the 7x7 value (2.57 ± 0.03)Å and the 1x1 value (2.64 ± 0.03)Å and is therefore < 0.1 Å. This is in agreement with recent channeling data /21/ but in contradiction with other UHV XSW measurements /7/ which found a contraction of 0.5 Å inward. Assuming a dimer-adatom-stacking fault model /22/ for the 7x7 unit cell, which was also used successfully to explain recent XSW results for Ge on Si(111) 7x7 /23/, the maximum coverage for adsorption on surface atop sites is 0.12 ML. Since much larger coherent coverages were measured with maximum f_c values, the surface adatoms must have been displaced from their sites to allow for more Br adsorption at surface ontop sites. This displacement is reflected in the change of the LEED pattern. The originally 7x7 unit cell is reordered in the interior similar to the cases of H /17/ and Cl /18/ adsorption. A possible explanation is the removal of the adatoms and survival of the dimers and the stacking fault. The small difference between the value after reordering, (2.54 ± 0.03)Å, and the pure 1x1, (2.64 ± 0.03)Å, case hints towards an inward relaxation albeit a small one.

The increase of the phase value for consecutive Br adsorption on a 1x1 surface can be interpreted by assuming an increasing ionic character of the Br-Si bonding. For this case the bondlength can be approximated by /19/

$$d_{cov/ion} = d_{cov} - b \log p \qquad (7)$$

where $p = v_a/n$ is the bonding number, with the effective valency v_a and the number of nearest neighbours n, and the empirical constant $b = 0.8$ Å /20/. The value $d_{cov/ion} = 2.73$ Å is calculated with an effective valency $v_a = 3$ and a coordination number $n = 4$, which is quite suitable for the high coverage Br case assuming that one Br is surrounded by three other Br atoms and one Si atom. This takes the interaction between adjacent Br atoms into account and its valency will thus differ from that of an isolated atom. Although the value from (7) cannot be taken as being precise because of the transfer of b from other bonding geometries and because of the rough description of the bonding by a number p, the measured increase of the position with coverage is explained by this model. Another possible explanation, namely an increasing outward relaxation of the top Si layer is much less unlikely, because this requires an increasing Si-Si bondlength. In addition, the lengthening of the bonding, because of the increased Br-Br interaction, also explains that the chemical preparations /2-4/ could only attain a maximum Θ_c of 0.20 ML. As discussed in /14,6/, the steric overlap of adjacent Br atoms will cause a change in bonding geometry and will increase the bonding energy which prohibits a higher Θ_c during deposition from the solution.

The threefold ionic site, which has been found /5/ on a differently prepared UHV surface before, did not show up in our present systematic study. This can be caused by a different method used for preparation here or by different Si materials with higher contaminent concentration.

Summary

The present XSW study on Br adsorbed on Si(111) for different reconstruction structures 1x1 and 7x7 has clearly shown that Br is adsorbed on the surface atop site in UHV just as it is known to be adsorbed on chemically prepared surfaces. With increasing coverage of Br on 1x1, the Si-Br bondlength increases because of the increasing Br-Br layer interaction. On a 7x7 surface, Br reorders the interior of the unit cell by a local reconstruction. No

indication was found for a large relaxation of the Si-Br double layer perpendicular to the bulk (111) diffraction planes.

Acknowledgement

The financial support of this project by the German Federal Minister for Science and Technology is gratefully acknowledged.

References

*now at: Hauni-Werke Körber & Co.KG, Kampchaussee 8-30, 2050 Hamburg 80, FRG

1. M.J. Bedzyk, W.M. Gibson and J.A. Golovchenko, J. Vac. Sci. Technol. 20 (1982) 634.
2. J.A. Golovchenko, J.R. Patel, D.R. Kaplan, P.L. Cowan and M.J. Bedzyk, Phys. Rev. Lett. 49 (1982) 560.
3. G. Materlik, A. Frahm and M.J. Bedzyk, Phys. Rev. Lett. 52 (1984) 441.
4. G. Materlik and J. Zegenhagen, Phys. Lett. 104A (1984) 47.
5. P. Funke and G. Materlik, Sol. Stat. Comm. 54 (1985) 921.
6. B.N. Dev, V. Aristov, N. Hertel, T. Thundat and W.M. Gibson, Surf. Sci. 163 (1985) 457.
7. S.M. Durbin, L.E. Berman, B.W. Batterman, and J.M. Blakely, Phys. Rev. Lett. 56, 236 (1986).
8. N. Hertel, G. Materlik and J. Zegenhagen, Z. Physik B - Condensed Matter 58 (1985) 199.
9. G. Materlik, Z. Physik B - Condensed Matter 61 (1985) 405.
10. P. Funke, G. Materlik and A. Reimann, Nucl. Instr. Meth. A246, 763 (1986).
11. P. Bennet and M.W. Webb, Surf. Sci. 104 (1981) 74.
12. C. Bendorf and B. Krüger, Surf. Sci. (in press).
13. J. Zegenhagen, G. Materlik and W. Uelhoff (in preparation).
14. M.J. Bedzyk and G. Materlik, Phys. Rev. B31 (1985) 4110.
15. CRC Handbook of Chemistry and Physics, CRC Press Inc., Boca Raton, Florida (1983).
16. S.M. Mohapatra, N. Sahoo, K.C. Mishra, B.N. Dev, W.M. Gibson, T.P. Das, Bull. Am. Phys. Soc., March 1985; see also J. Vac. Sci. Technol. (in press).
17. E.G. McRae and C.W. Caldwell, Phys. Rev. Lett. 46 (1981) 1632.
18. R.D. Schnell, D. Rieger, A. Bogen, F.J. Himpsel, K. Wandelt and W. Steinmann, Phys. Rev. B32, 8057 (1985).
19. L. Pauling, "Die Natur der chemischen Bindung", Verlag Chemie, Weinheim, 1973.
20. K.A.R. Mitchell, Surf. Sci. 155 (1985) 93.
21. R.M. Tromp, J. Vac. Sci. Technol. A1 (1983) 1047.
22. K. Takayanagi, Y. Tanishiro, M. Takahashi and S. Takahashi, J. Vac. Sci. Technol. A3 (1985) 1502.
23. B.N. Dev, G. Materlik, R.L. Johnson, F. Grey and M. Clausnitzer, Phys. Rev. Lett. 57, 3058 (1986).

Table 1

XSW results from different areas of a sample at different times after preparation.

Φ	f_c	comment
0.85 ± 0.02	0.78 ± 0.06	sample area fully exposed, directly after preparation of Br adsorbate
0.85 ± 0.03	0.33 ± 0.06	only central area of the beam, no edge regions included, ~ 1-2 h after preparation
0.84 ± 0.02	0.30 ± 0.05	slit seize further reduced, ~ 2-7 h after preparation
0.91 ± 0.03	0.16 ± 0.04	area close to sample edge exposed, ~ 8-12 h after preparation

Table II

Sequence of coverage dependent standing wave measurements on Si(111)1x1.

Q_{el} (mA min)	σ_{fl} (10^{14}/cm^2)	Θ (ML)	Φ	f_c	$d_{Br-(111)}$ (Å)	Θ_c
40	2.3	0.33	0.84 ± 0.02	0.24 ± 0.03	2.64	0.08
80	3.3	0.47	0.87 ± 0.02	0.26 ± 0.03	2.73	0.12
120	3.4	0.49	0.88 ± 0.02	0.35 ± 0.02	2.76	0.17
240	4.5	0.64	0.89 ± 0.02	0.27 ± 0.02	2.79	0.17
360	6.8	0.96	0.88 ± 0.01	0.30 ± 0.02	2.76	0.29
480	6.4	0.91	0.88 ± 0.01	0.37 ± 0.02	2.76	0.39
720	6.7	0.96	0.87 ± 0.01	0.35 ± 0.02	2.73	0.34

Q_{el} is the electric charge released from the AgBr cell. σ_{fl} is the Br coverage estimated from the ratio of Si and Br K_α fluorescence yields. Θ is the corresponding Br coverage in parts of a monolayer. The measured saturation coverage at approximately 7×10^{14}/cm^2 has been set to $\Theta = 1$. The theoretical value of 7.83×10^{14}/cm^2 is within the error limit of ~ 10 %. $d_{Br-(111)} = \Phi \times 3.14$ Å. See text for definition of Φ, f_c and Θ_c.

Table III

List of distances of the Br atom from the top Si layer as calculated and measured with different methods (see text).

	$d_{Br-(111)}$ (Å)
from $SiBr_4$ /15/	2.54
from covalent radii	2.70
cluster calculation /16/	2.62
d_{cov} from /6/	2.64
$d_{cov/ion}$ from (7)	2.73
chemical preparation /4/	2.61 ± 0.01
this work:	
UHV 1x1 low cov.	2.64 ± 0.03
large cov.	2.76 ± 0.03
UHV 7x7 Br	2.57 ± 0.03
UHV 1x1 (annealed 7x7 Br)	2.54 ± 0.03

Figure Captions

Figure 1 Experimental arrangement (schematic). SR: synchrotron radiation; P1, P2: piezoelectric transducers; c: capacitive distance pick-up; I_1: ionisation chamber.

Figure 2 Rocking curves of a Si(111) reflection. ●●●: perfect reflection curves; ■■■: reflectivity curve after sample sputtering.

Figure 3 Non-dispersive Si(111) double crystal topographs. Monochromator: 1. crystal Si(111) symmetric, 2. crystal Si(111) asymmetric, 7° between surface plane and (111) planes. E_γ = 15 keV. A shadow is visible from the Br source. The bottom picture shows a homogeneous reflection. The width of each top row reflection corresponds to about 1 cm.

Figure 4 Auger electron spectra. ——: right after sample insertion into the UHV from an etch bath. ---: after sputtering and annealing.

Figure 5 Experimental (x, ⧫) and theoretical (---, ——) reflectivity and Br K_α fluorescence curves from a Br/Si(111) 1x1 reflection.

Figure 6 Experimental and theoretical Si(111) reflectivity curve (x, ---) and the corresponding Br K_α fluorescence yield curves of a Br layer before (⧫, ——) and after (⧫, -·-·) thermal annealing.

Figure 7 Experimental and theoretical Si(111) reflecitvity curve (x, ---) and the corresponding Br K_α fluorescence yield curves of a Br layer after direct deposition onto a 7x7 surface (⧫, ——) and after consecutive tempering (⧫, -·-·). The 7x7 curve is shifted upwards by 0.4 units.

FIG. 1

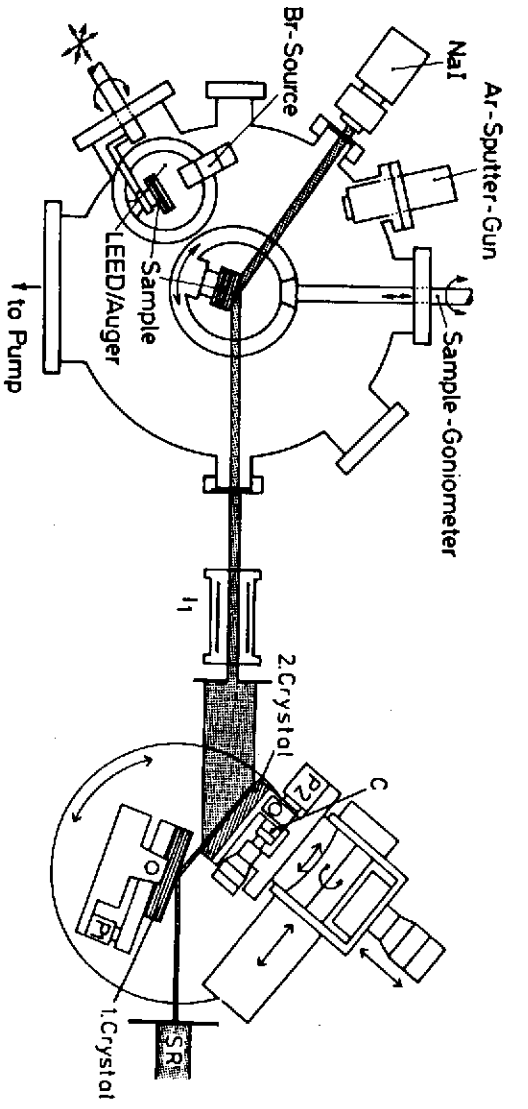

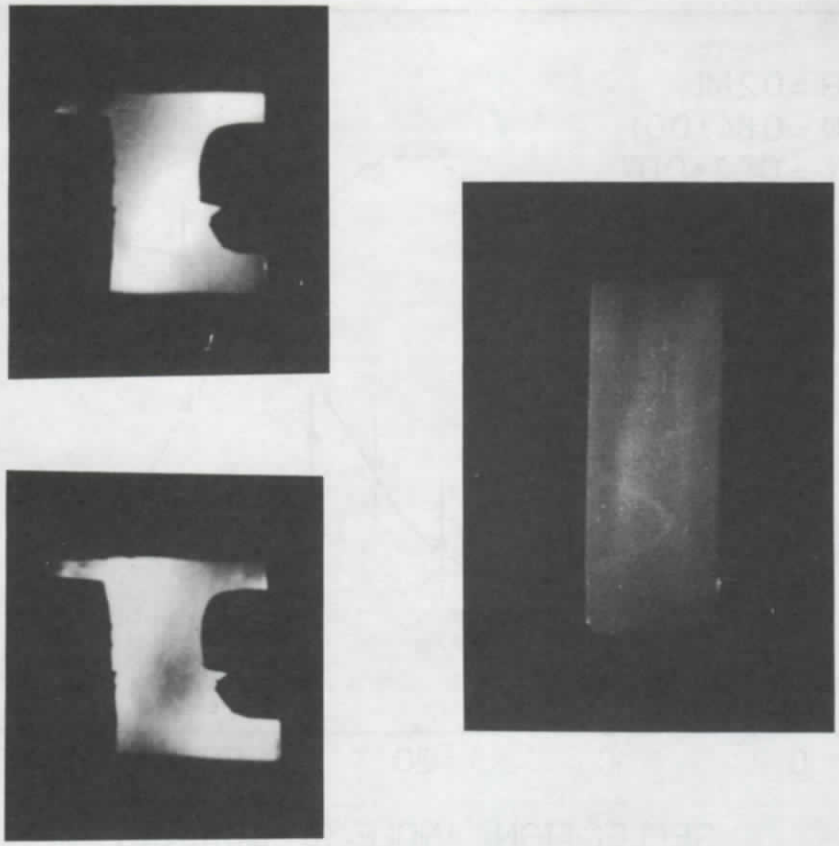

FIG. 3

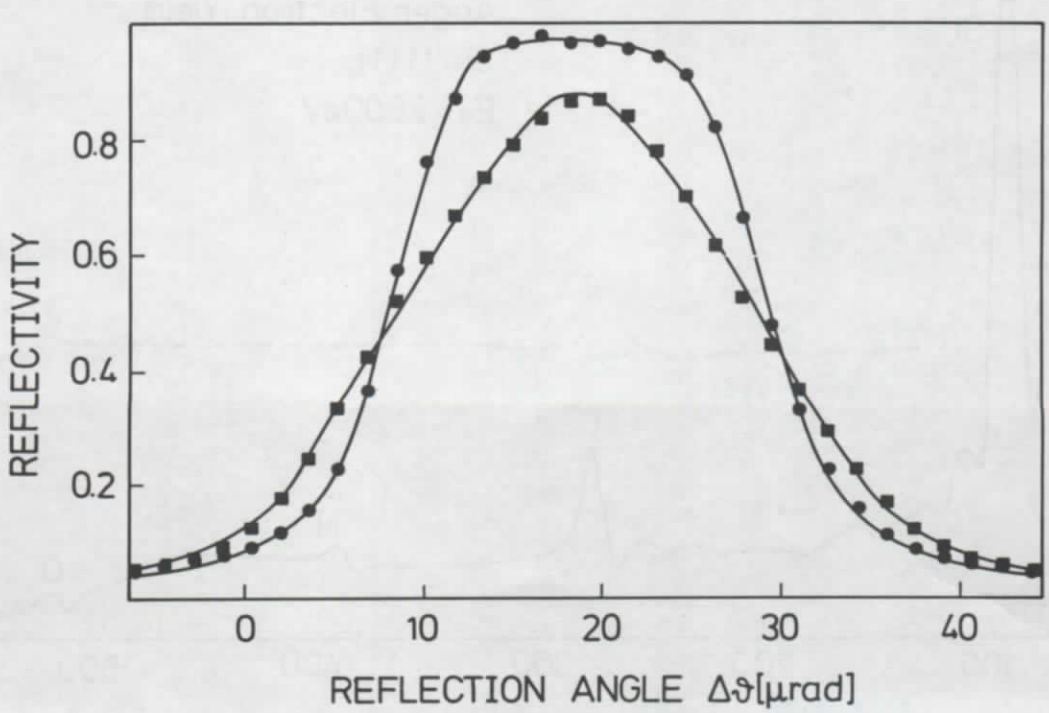
REFLECTIVITY
0.8
0.6
0.4
0.2
0
10
20
30
40
REFLECTION ANGLE Δϑ[μrad]

FIG. 2

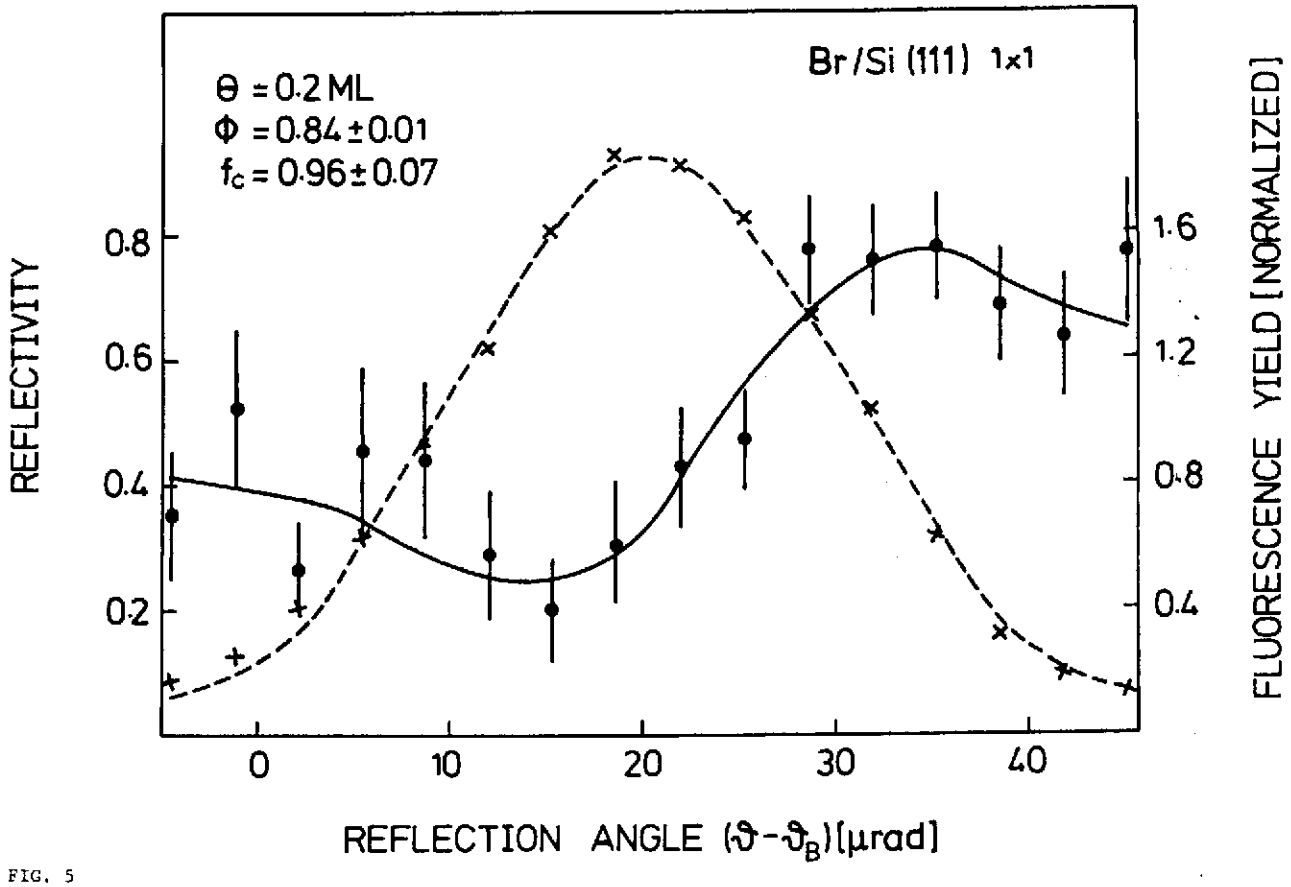
Br/Si (111) 1×1
Θ = 0.2 ML
Φ = 0.84 ± 0.01
f_c = 0.96 ± 0.07
REFLECTIVITY
FLUORESCENCE YIELD [NORMALIZED]
0.2
0.4
0.6
0.8
0.4
0.8
1.2
1.6
0
10
20
30
40
REFLECTION ANGLE (ϑ - ϑB) [μrad]

FIG. 5

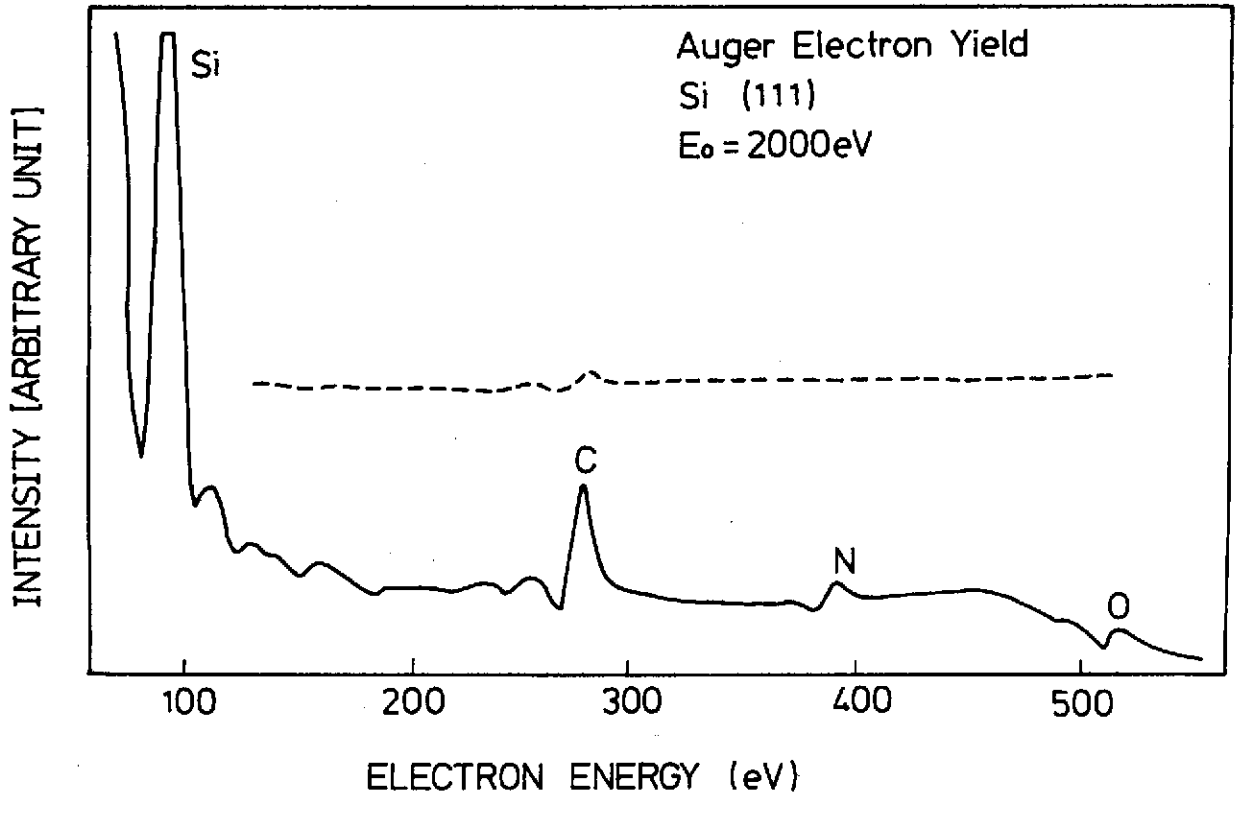
Auger Electron Yield
Si (111)
E₀ = 2000eV
Si
C
N
O
INTENSITY [ARBITRARY UNIT]
100
200
300
400
500
ELECTRON ENERGY (eV)

FIG. 4

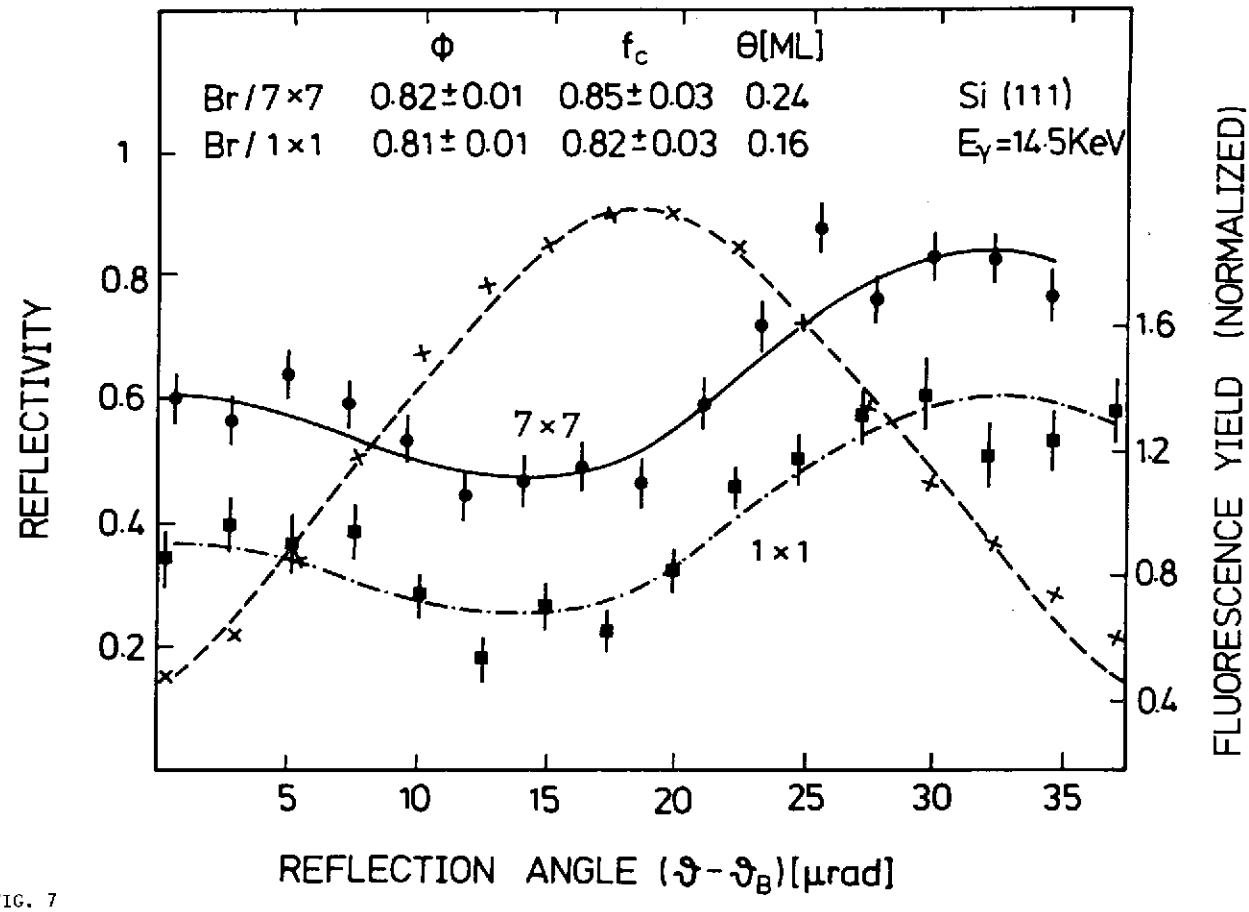
Φ
f_c
θ[ML]
Br/7×7 0.82±0.01 0.85±0.03 0.24
Br/1×1 0.81±0.01 0.82±0.03 0.16
Si (111)
E_γ=14.5KeV
7×7
1×1
REFLECTIVITY
FLUORESCENCE YIELD (NORMALIZED)
REFLECTION ANGLE (ϑ-ϑB) [μrad]

FIG. 7

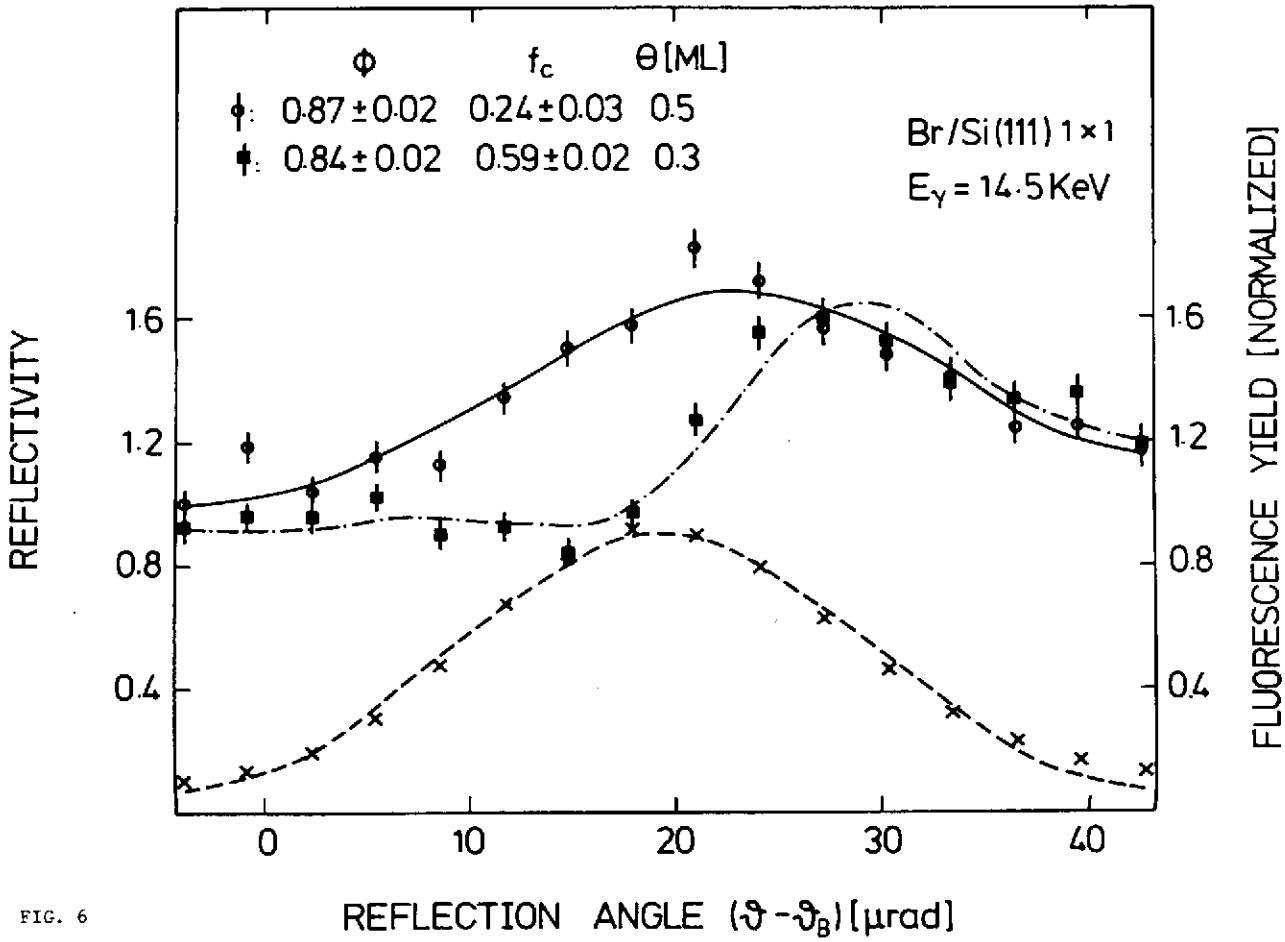
Φ
f_c
θ[ML]
0.87±0.02 0.24±0.03 0.5
0.84±0.02 0.59±0.02 0.3
Br/Si(111) 1×1
E_γ = 14.5 KeV
REFLECTIVITY
FLUORESCENCE YIELD (NORMALIZED)
REFLECTION ANGLE (ϑ-ϑB) [μrad]

FIG. 6